

# Robust adaptive fault-tolerant control for path maneuvering of autonomous surface vehicles with actuator faults based on the noncooperative game strategy

Yibo Zhang<sup>a</sup>, Di Wu<sup>a,b</sup>, Peng Cheng<sup>a</sup>, Wentao Wu<sup>a</sup>, Weidong Zhang<sup>a,b,\*</sup>

<sup>a</sup> Department of Automation, Shanghai Jiao Tong University, Shanghai 200240, China

<sup>b</sup> School of Information and Communication Engineering, Hainan University, Haikou, 570228, Hainan, China

## ARTICLE INFO

### Keywords:

Path maneuvering  
Autonomous surface vehicle (ASV)  
Noncooperative game  
Actuator faults  
Concurrent learning

## ABSTRACT

This paper investigates a parameterized path-guided following/maneuvering control problem of an autonomous surface vehicle (ASV) subject to actuator faults via a noncooperative game strategy. Unlike the existing path maneuvering control methods, the noncooperative game of this paper includes two sub-games. On one hand, the path update is considered to be against the effort of kinematic control. On the other hand, the kinetic control is considered to be against the total disturbances consisting of actuator faults and external disturbances. A robust adaptive fault-tolerant path maneuvering controller is designed based on a noncooperative game approach. Specifically, we design a kinematic control law using an improved dynamic surface control approach to achieve the geometric objective. An improved neural predictor is constructed, in which a concurrent learning-based adaptation is designed to identify unknown fault coefficients. A path update law and a kinetic control law are calculated to cover noncooperative games by using an adaptive dynamic programming approach. Theoretical analysis shows that the closed-loop system is input-to-state stable, and the proposed method can meet the geometric objective, the dynamic objective, and the fault-tolerant objective. Finally, simulation results demonstrate the efficacy of the proposed robust adaptive fault-tolerant control method for path maneuvering.

## 1. Introduction

Autonomous surface vehicle (ASV) is a kind of intelligent marine robot and can replace humans in many maritime operations (Gu et al., 2022a,b; Wang et al., 2024). Motion control remains a significant topic for the ASV as it provides the most fundamental assurance during naval operations. In recent two decades, many motion control methods have been proposed for the ASV, including target tracking (Ma et al., 2022; Gao et al., 2021; Hu and Zhang, 2022; Gao et al., 2023), trajectory tracking (Ma et al., 2019; Wu et al., 2022a,b; He et al., 2023), and path following/maneuvering (Skjetne et al., 2004, 2005; Zhang et al., 2017, 2022; Liu et al., 2020; Lv et al., 2023, 2022; Peng et al., 2018, 2020; Gu et al., 2021; Zhang et al., 2021, 2023). Similar to trajectory tracking and target tracking, path maneuvering is also to drive vehicles to move along a given path at the geometric level. But different from trajectory and target tracking, there exists an additional path variable as a free degree of control in each given path, in which a dynamic task should be considered for path update via tuning this variable during path maneuvering. In Skjetne et al. (2004), a robust maneuvering control method

is proposed. In Skjetne et al. (2005), an adaptive path maneuvering controller is designed for a model ship with experimental validations. In Zhang et al. (2017), a waypoints-based path maneuvering controller is constructed based on a robust neural adaptation. In Zhang et al. (2022), an event-based control method is developed for path maneuvering of underactuated surface vehicles, and an event-triggered mechanism with the dynamic threshold is designed. Moreover, some path maneuvering control methods have been proposed for multiple vehicles, such as decentralized cooperative maneuvering (Liu et al., 2020; Lv et al., 2023, 2022), formation maneuvering (Peng et al., 2018, 2020), distributed containment maneuvering (Gu et al., 2021; Zhang et al., 2021), and noncooperative game-based distributed maneuvering (Zhang et al., 2023). These interesting results in Skjetne et al. (2004, 2005), Zhang et al. (2017, 2022), Liu et al. (2020), Lv et al. (2023, 2022), Peng et al. (2018, 2020), Gu et al. (2021), Zhang et al. (2021) and Zhang et al. (2023) only consider the desired path update, which the path variable is driven to satisfy given dynamic assignments. However, as an additional free degree of control, the path

\* Corresponding author.

E-mail addresses: [zhang297@sjtu.edu.cn](mailto:zhang297@sjtu.edu.cn) (Y. Zhang), [wentao-wu@sjtu.edu.cn](mailto:wentao-wu@sjtu.edu.cn) (W. Wu), [wdzhang@sjtu.edu.cn](mailto:wdzhang@sjtu.edu.cn) (W. Zhang).

variable is linked with the kinematic control level of the ASV and can reduce the effort of kinematic control via a specific update law (Dacic et al., 2006). In other words, there exists a game between the path update and the kinematic control. Besides, these meaningful results in Skjetne et al. (2004, 2005), Zhang et al. (2017, 2022), Liu et al. (2020), Lv et al. (2023, 2022), Peng et al. (2018, 2020), Gu et al. (2021), Zhang et al. (2021) and Zhang et al. (2023) is under an ideal actuator condition. However, the actuators of the ASV are easily subject to faults in applications due to unexpected aging and wear (Jin, 2016).

Many fault-tolerant control methods have been proposed for marine vehicles (Jin, 2016; Hao et al., 2020; Zhu et al., 2023; Lu et al., 2021; Wu and Tong, 2023). In Jin (2016), a fault-tolerant control scheme is designed for the formation of underactuated autonomous surface vessels, and time-varying tan-type barrier Lyapunov functions are introduced to cover line-of-sight range and angle constraints. In Hao et al. (2020), a slide mode fault-tolerant controller is designed for marine surface vehicles subject to time delay. In Zhu et al. (2023), an event-triggered adaptive PID-type controller is developed for fault-tolerant control of underactuated ships, and state saturation is also considered. In Lu et al. (2021), a robust adaptive fault-tolerant control method is proposed for cooperative control of multiple unmanned surface vehicles, and both the known fault case and the unknown fault case are investigated. Furthermore, output-feedback fault-tolerance is addressed for marine vehicles subject to immeasurable states in Wu and Tong (2023). It should be noted that these meaningful results on fault-tolerance of marine vehicles (Jin, 2016; Hao et al., 2020; Zhu et al., 2023; Lu et al., 2021; Wu and Tong, 2023) consider the compensating or counteracting mechanism for actuator faults. In the last two years, a new fault-tolerant control method has been proposed in Ren et al. (2022), Ma et al. (2023) by introducing a noncooperative game theory. In the noncooperative game, the kinetic control and the actuator fault can be treated as two players. The competitive relationships of these two players can be modeled as a convex payoff function, and the optimal kinetic control law and the worst actuator fault can be constructed by solving this payoff function.

The model of the ASV is in the presence of uncertain nonlinearities caused by unmodeled dynamics and unknown parameters. In many path maneuvering control designs, the neural predictor is designed as approximators to identify these uncertain nonlinearities (Liu et al., 2020; Lv et al., 2023, 2022; Peng et al., 2018, 2020; Gu et al., 2021). Compared with the traditional neural network adaptation, neural predictors can improve the transient performance of neural approximation by using a predicted error as a tuning term in the adaptation law. Besides, some improved neural predictors have been proposed, such as high-order tuner-based neural predictor (Zhang et al., 2023) and finite-time neural predictor (Jiang et al., 2023). However, when the actuator faults occur, these neural predictors may not be directly applicable in fault-tolerant control design. This is because the actual kinetic control law is not equal to the ideal control input during a fault. Therefore, it is rewarding to further improve the neural predictor for the fault-tolerant path maneuvering problem.

This paper aims to investigate the path maneuvering problem of an ASV. The dynamics of the ASV is subject to internal uncertainties and external disturbances. Besides, the vehicle is also subject to actuator faults. A robust adaptive fault-tolerant controller, consisting of a kinematic control law, a path update law, an improved neural predictor, and a kinetic control law, is designed for path maneuvering of the ASV based on a noncooperative game strategy. The noncooperative game herein includes two aspects. The desired path update and the effort of kinematic control can be regarded as a game, and the kinetic control, the external environmental disturbances, and the actuator faults can be also taken as a game. In contrast to the existing results on path maneuvering and fault-tolerant control of marine vehicles, the main contributions of this paper are as follows.

- Compared with the existing path maneuvering control methods in Skjetne et al. (2004, 2005), Zhang et al. (2017, 2022), Liu et al. (2020), Lv et al. (2023, 2022), Peng et al. (2018, 2020), Gu et al. (2021), Zhang et al. (2021) and Zhang et al. (2023) for the ASV, we propose a noncooperative game-based variable tuning law for path update herein. The relationship between kinematic control and path update is considered as a dynamic game. The proposed variable tuning law is to reduce the kinematic control effort and achieve the desired path update.
- Different from fault-tolerant control methods for marine vehicles in Jin (2016), Hao et al. (2020), Zhu et al. (2023), Lu et al. (2021) and Wu and Tong (2023), the proposed fault-tolerant control method herein is based on a noncooperative game strategy, in which the actuator fault and the kinetic control is considered as a dynamic game. The kinetic control law is obtained by calculating the payoff function among kinetic control and total disturbances.
- Compared with the neural predictor design in Liu et al. (2020), Lv et al. (2023, 2022), Peng et al. (2018, 2020), Gu et al. (2021), Zhang et al. (2023) and Jiang et al. (2023) for path maneuvering, an improved neural predictor is developed based on the concurrent learning approach, which unknown fault coefficients can be identified. The approximation of the neural network is less affected by the actuator fault. Therefore, the improved neural predictor is more suitable for the actuator fault case.

The remainder of this paper is organized as below. We introduce some related preliminaries and give the problem formulation briefly in Section 2. The design process of the robust adaptive fault-tolerant controller is given in Section 3. The main theoretical results of this paper are analyzed in Section 4. Simulation examples are provided to illustrate the effectiveness of the proposed method in Section 5. At last, we conclude this paper in Section 6.

*Notation:* Define  $\lambda_{\min}(\cdot)$  and  $\lambda_{\max}(\cdot)$  as the minimal and maximal eigenvalue value of a matrix respectively,  $\mathbb{R}^n$  as the  $n$ -dimensional Euclidean space,  $\mathbb{R}^+$  as the set of positive real number,  $\|\cdot\|$  as the Euclidean norm of a vector and the Frobenius norm a matrix.

## 2. Preliminaries and problem formulation

The model of the ASV is described by the following form

$$\begin{cases} \dot{\eta} = R(\psi)v \\ R(\psi) = \begin{bmatrix} \cos(\psi) & -\sin(\psi) & 0 \\ \sin(\psi) & \cos(\psi) & 0 \\ 0 & 0 & 1 \end{bmatrix} \\ M\dot{v} = \tau + f(v) + w(t) \end{cases} \quad (1)$$

where  $\eta = [x, y, \psi]^T \in \mathbb{R}^3$  with  $x, y$  being the positions in the north-east-down frame and  $\psi$  being a heading angle,  $v = [u, v, r]^T \in \mathbb{R}^3$  is a vector that encompasses the velocities of surge, sway, and yaw in the body-fixed frame,  $M = \text{diag}\{m_u, m_v, m_r\} \in \mathbb{R}^{3 \times 3}$  is an internal parameter matrix,  $f(v) \in \mathbb{R}^3$  denotes a collection of uncertain nonlinear terms produced by various factors such as Coriolis and centripetal forces, hydrodynamics, unknown damping, and unmodeled dynamics,  $\tau = [\tau_u, \tau_v, \tau_r]^T \in \mathbb{R}^3$  with  $\tau_u, \tau_v$  being the torques and  $\tau_r$  being the moment, and  $w(t) \in \mathbb{R}^3$  is a time-varying bounded environmental disturbance.

It can be observed that the dynamics of the ASV is modeled in the two different frames. We can transform (1) into the following form in the north-east-down frame

$$\begin{cases} \dot{\eta} = \bar{v} \\ \dot{\bar{v}} = M^{-1}\bar{\tau} + \bar{f}(v) + \bar{w}(t) \end{cases} \quad (2)$$

where  $\bar{v} = R(\psi)v = [\bar{u}, \bar{v}, \bar{r}]^T$ ,  $\bar{f}(v) = \dot{R}(\psi)v + R(\psi)M^{-1}f(v)$ ,  $\bar{\tau} = [\tau_x, \tau_y, \tau_r]^T \in \mathbb{R}^3$  with  $\tau_x = \cos(\psi)\tau_u + \sin(\psi)\tau_v$ ,  $\tau_y = \sin(\psi)\tau_u + \cos(\psi)\tau_v$ , and  $\bar{w}(t) = R(\psi)M^{-1}w(t)$ .

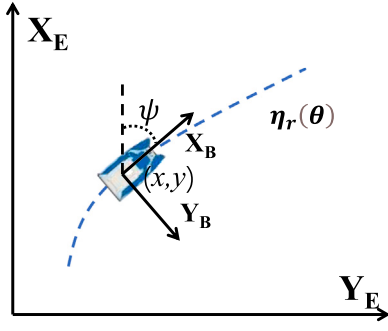


Fig. 1. Illustration of path maneuvering of the ASV.

In this paper, the actuator fault consists of the actuator bias and the loss of effectiveness. The model of the actuator fault can be expressed by the following form

$$\bar{\tau} = \sigma \tau_a + \tilde{\tau}(t) \quad (3)$$

where  $\tau_a = [\tau_{a,u}, \tau_{a,v}, \tau_{a,r}]^T \in \mathbb{R}^3$  denote the actual control input,  $\sigma = \text{diag}\{\sigma_u, \sigma_v, \sigma_r\} \in \mathbb{R}^{3 \times 3}$  with  $\sigma_u, \sigma_v, \sigma_r \in (0, 1)$  denotes an unknown fault pattern matrix and  $\tilde{\tau}(t) \in \mathbb{R}^3$  is the actuator bias. when  $\sigma_l < 1$  with  $l = u, v, r$  means the  $l$ th actuator is subject to partial effectiveness losses and  $\sigma_l = 1$  means the  $l$ th actuator can control freely. Merging (3) into (2), the model of the ASV subject to the unexpected actuator fault is rewritten as follows

$$\begin{cases} \dot{\eta} = \bar{v} \\ \dot{v} = M^{-1}(\sigma \tau_a + \tilde{\tau}(t)) + \bar{f}(v) + \bar{w}(t). \end{cases} \quad (4)$$

This paper is to design a robust adaptive fault-tolerant controller for path maneuvering of the ASV subject to uncertainties, external disturbances, and unexpected actuator faults. The ASV can achieve the following geometric task, dynamic task, and fault-tolerant task through the use of the proposed controller. Illustration of path maneuvering is shown in Fig. 1.

- **Geometric Objective:** The output trajectory  $\eta$  of the ASV is driven to follow a desired parameterized path as far as possible. The mathematic process is given as follows.

$$\|\eta - \eta_r(\theta)\| \leq \iota_g \quad (5)$$

where there exists a residual error  $\iota_g \in \mathbb{R}^+$ .

- **Dynamic Objective:** The path update law  $\omega$  is considered as an action of a player during the noncooperative game. This player is driven to minimize a convex payoff function associated with the kinematic control and path update. The mathematic process is described as follows.

$$\min J_d(\omega, z_d). \quad (6)$$

- **Fault-tolerant Objective:** The kinetic control law  $\tau_a$  is considered as an action of a player during the noncooperative game. This player is driven to minimize a convex payoff function associated with the kinetic control and fault-tolerance. The mathematics process is

$$\min J_v(z_v, \tau_a, w_{\text{tot}}). \quad (7)$$

Several assumptions will be required throughout this paper.

**Assumption 1.** Parameterized path  $\eta_r(\theta)$  and its velocity  $\dot{\eta}_r(\theta)$  are smooth and bounded, i.e.  $\|\eta_r(\theta)\| \leq \eta_r^*$  and  $\|\dot{\eta}_r(\theta)\| \leq \dot{\eta}_r^*$  with  $\eta_r^*, \dot{\eta}_r^* \in \mathbb{R}^+$ .

**Assumption 2.** External disturbance is bounded, i.e.  $\|\bar{w}(t)\| \leq w^*$  with  $w^* \in \mathbb{R}^+$ .

**Assumption 3.** Actuator bias is bounded, i.e.  $\|\tilde{\tau}(t)\| \leq \tilde{\tau}^*$  with  $\tilde{\tau}^* \in \mathbb{R}^+$ .

**Remark 1.** Assumption 1 is common in many existing results (Gu et al., 2022a; Liu et al., 2021) because we always plan a smooth and bounded path described by mathematics. It is convenient for the ASV to design controllers. Assumption 2 is realistic for practical applications because we cannot always use the ASV in inclement weather. Assumption 2 can be founded in existing results, such as Gu et al. (2022a), Liu et al. (2021) and Peng et al. (2020). Assumption 3 provides a reasonable condition for the structural features of actuators. If the bias is too large, the actuator bias is the same as the loss of effectiveness. Assumption 3 is common in existing fault-tolerant control methods, such as Ren et al. (2022), Ma et al. (2023) and Lu et al. (2021).

### 3. Robust adaptive fault-tolerant controller design for path maneuvering of the ASV

In the previous section, we introduce the model of the ASV and three control objectives of path maneuvering. We construct a robust adaptive fault-tolerant controller for path maneuvering in this section. The proposed controller is modular and under a noncooperative game strategy, including a kinematic control law, a path update law, an improved neural predictor, and a kinetic control law. The kinematic control law and the path update law are at the kinematic level, and the improved neural predictor and the kinetic control law are at the kinetic level.

#### 3.1. Kinematic control law and path update law design at the kinematic level

In this subsection, the kinematic control is considered. A kinematic control law is developed based on a dynamic surface control approach. Besides, the path update is closely connected with the kinematic control, and thus we design a path update law for the path variable via utilizing this connection.

*Step 1.* In this step, a kinematic control law is constructed for the ASV to track the desired parameterized path. Firstly, define a kinematic tracking error  $z_1 = \eta - \eta_r(\theta)$ . The dynamics of  $z_1$  along (4) can be calculated as  $\dot{z}_1 = \bar{v} - \dot{\eta}_r(\theta)$ . To stabilize  $\dot{z}_1$ , we can design a kinematic control law as below

$$\alpha = -K_1 z_1 + \dot{\eta}_r(\theta) \quad (8)$$

where  $K_1 = \text{diag}\{k_x, k_y, k_\psi\}$  with  $k_x, k_y, k_\psi \in \mathbb{R}^+$  being the control gain in each degree of freedom. Then, let  $\alpha$  pass through the following nonlinear tracking differentiator

$$\begin{cases} \dot{v}_a = v_a^d \\ \dot{v}_a^d = -\gamma_a^2 \left[ \beta_{a,1} (v_a - \alpha)^{\frac{1}{2}} + \beta_{a,2} \left( \frac{v_a^d}{\gamma_a} \right)^{\frac{2}{3}} \right] \end{cases} \quad (9)$$

where  $v_a \in \mathbb{R}^3$  can be considered as an estimation of  $\alpha$ ,  $\gamma_a \in \mathbb{R}^+$  is a time constant of the differentiator,  $\beta_{a,1}, \beta_{a,2} \in \mathbb{R}^+$  are two tuning parameters. Ref. Guo and Zhao (2011) has shown that both  $\|v_a - \alpha\|$  and  $\|\dot{v}_a - \dot{\alpha}\|$  are bounded.

*Step 2.* The desired parameterized path  $\eta_r(\theta)$  contains a path variable  $\theta$ , which is as an additional control degree of freedom. Therefore, a path update law is essential. At first, consider the dynamics of  $\theta$  as  $\dot{\theta} = \omega$ . Then, the kinematic control law designed in the previous step can be rewritten as follows

$$\alpha = -K_1 z_1 + \frac{\partial \eta_r(\theta)}{\partial \theta} \omega. \quad (10)$$

In path maneuvering, the term  $(\partial \eta_r(\theta) / \partial \theta) \omega$  can be used to design a scheme for  $\omega$  to reduce the control effort of (8). That is to say, there exists a noncooperative game, which  $\omega$  and  $\alpha$  can be considered as two players. Besides, as the dynamics of the path variable  $\theta$ ,  $\omega$  is also employed to achieve desired path update. Illustration of noncooperative game between path update and kinematic control is shown in Fig. 2.

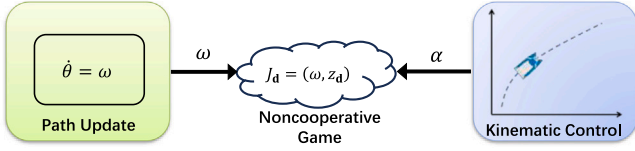


Fig. 2. Illustration of noncooperative game between path update and kinematics control.

We can construct the following convex payoff function to describe this game

$$J_d(\omega, z_d) = \int_0^\infty \left( \left\| -K_1 z_1 + \frac{\partial \eta_r(\theta)}{\partial \theta} \omega \right\|^2 + c_d(\omega + k_d z_d)^2 \right) dt \quad (11)$$

where  $k_d \in \mathbb{R}^+$  and  $c_d \in \mathbb{R}^+$  are two tuning parameters, and  $z_d = \theta - \int v_s dt$  denotes a tracking error for the dynamic objective.

Along the payoff function (11), we try to find an optimal  $\omega$  as far as possible. Another player  $\alpha$  is considered to be independent. The mathematics process is expressed as follows

$$J_d^* = \min_{\omega} J_d(\omega, z_d). \quad (12)$$

There exists a Nash equilibrium  $\omega^*$  in this game, such that the following inequality is satisfied

$$J_d(\omega^*) \leq J_d(\omega). \quad (13)$$

Then, the Hamiltonian function associated with (11) is expressed as follows

$$H_d(\omega, z_d, \nabla J_d(z_d)) = \left\| -K_1 z_1 + \frac{\partial \eta_r(\theta)}{\partial \theta} \omega \right\|^2 + c_d(\omega + k_d z_d)^2 + \nabla J_d(z_d)(\omega - v_s). \quad (14)$$

A Hamilton–Jacobi–Isaacs (HJI) function is obtained as

$$0 = \min_{\omega} H_d(\omega, z_d, \nabla J_d(z_d)). \quad (15)$$

Taking the partial derivative of the above HJI function, we have the following condition

$$\frac{\partial H_d}{\partial \omega} = 0. \quad (16)$$

Then, the optimal path update law  $\omega^*$  can be obtained along (14) as follows

$$\omega^* = -\frac{2c_d k_d z_d + 2 \left( \frac{\partial \eta_r(\theta)}{\partial \theta} \right)^T Y_a + \nabla J_d^*(z_d)}{2 \left( c_d + \left\| \frac{\partial \eta_r(\theta)}{\partial \theta} \right\|^2 \right)} \quad (17)$$

where  $Y_a = -K_1 z_1$ .

Obviously, we need to solve the HJI function  $H_d$  to obtain the optimal path update law  $\omega^*$ . But, HJI function is very hard to calculate by mathematical derivation. Therefore, an adaptive dynamic programming policy can be introduced to deal with this problem. Then, a critic neural network consisting of  $\rho_d$  neurons can be used to identify  $J_d^*$  as follows

$$J_d^*(z_d) = W_d^T \sigma_d(\zeta_d) + \varepsilon_d \quad (18)$$

where  $W_d \in \mathbb{R}^{\rho_d}$  is the weight vector of the critic neural network satisfying  $\|W_d\| \leq W_d^*$  with  $W_d^* \in \mathbb{R}^+$  being the upper bound,  $\sigma_d(\zeta_d) \in \mathbb{R}^{\rho_d}$  is the output vector of the hidden layer with  $\zeta_d$  being the input, and  $\varepsilon_d \in \mathbb{R}$  is the approximation error satisfying  $|\varepsilon_d| \leq \varepsilon_d^*$  with  $\varepsilon_d^* \in \mathbb{R}^+$  being the upper bound.

Then,  $\nabla J_d^*(z_d)$  is expressed by the following form

$$\nabla J_d^*(z_d) = \nabla \sigma_d^T(\zeta_d) W_d + \nabla \varepsilon_d \quad (19)$$

where  $\nabla \sigma_d(\zeta_d) = \partial \sigma_d(\zeta_d) / \partial z_d \in \mathbb{R}^{\rho_d}$  and  $\nabla \varepsilon_d = \partial \varepsilon_d / \partial z_d \in \mathbb{R}$ .

Substituting (19) into (17), we have

$$\omega^* = -\frac{2Y_d + (\nabla \sigma_d^T(\zeta_d) W_d + \nabla \varepsilon_d)}{2\Pi_d} \quad (20)$$

where  $Y_d = c_d k_d z_d + (\partial \eta_r(\theta) / \partial \theta)^T Y_a$ ,  $\Pi_d = (c_d + \|\partial \eta_r(\theta) / \partial \theta\|^2)$ .

Substituting (17) into (14), we have the following HJI approximation error

$$\begin{aligned} \delta_d = & \left\| Y_a + \left( \frac{\partial \eta_r(\theta)}{\partial \theta} \right)^T \left( \frac{2Y_d + (\nabla \sigma_d^T(\zeta_d) W_d)}{2\Pi_d} \right) \right\|^2 \\ & + c_d \left( \frac{2Y_d + (\nabla \sigma_d^T(\zeta_d) W_d)}{2\Pi_d} + k_d z_d \right)^2 \\ & + \nabla \sigma_d^T(\zeta_d) W_d \left( \frac{2Y_d + (\nabla \sigma_d^T(\zeta_d) W_d)}{2\Pi_d} - v_s \right). \end{aligned} \quad (21)$$

Because the real value of  $W_d$  cannot be obtained, an actual path update law  $\hat{\omega}$  is constructed by using the estimated information as follows

$$\hat{\omega} = -\frac{2Y_d + (\nabla \sigma_d^T(\zeta_d) \hat{W}_d)}{2\Pi_d} \quad (22)$$

where  $\hat{W}_d$  is an estimation of  $W_d$ .

An approximated Hamilton function is constructed as

$$\begin{aligned} e_d = & \left\| -K_1 z_1 - \left( \frac{\partial \eta_r(\theta)}{\partial \theta} \right)^T \frac{2Y_d + (\nabla \sigma_d^T(\zeta_d) \hat{W}_d)}{2\Pi_d} \right\|^2 \\ & + c_d \left( \frac{2Y_d + (\nabla \sigma_d^T(\zeta_d) \hat{W}_d)}{2\Pi_d} + k_d z_d \right)^2 \\ & + \nabla \sigma_d^T(\zeta_d) \hat{W}_d \left( \frac{2Y_d + (\nabla \sigma_d^T(\zeta_d) \hat{W}_d)}{2\Pi_d} - v_s \right). \end{aligned} \quad (23)$$

Define a squared residual error  $E_d$  as follows

$$E_d = \frac{1}{2} e_d^2. \quad (24)$$

An update law for  $\hat{W}_d$  can be constructed based on the gradient descent scheme as follows

$$\dot{\hat{W}}_d = -\left( \frac{\rho_d \varphi_d}{(1 + \varphi_d^T \varphi_d)^2} \right) \frac{\partial E_d}{\partial \hat{W}_d} \quad (25)$$

where  $\rho_d \in \mathbb{R}^+$  is an adaptation gain and  $\varphi_d = \nabla \sigma_d^T(\zeta_d)(\hat{\omega} - v_s)$ .

### 3.2. Neural predictor and kinetic control law design at the kinetic level

We have developed the kinematic control law and the path update law in the previous subsection. In this subsection, a control law is designed at the kinetic level based on a two-players noncooperative game to achieve fault tolerance. Besides, a neural predictor is also essential to approximate the uncertain dynamics of the ASV.

*Step 1.* Approximator is the premise of the kinetic control law. In this step, an improved neural predictor will be constructed to estimate the uncertain nonlinear term and identify unknown fault coefficients. At first, recall the kinetics of the ASV as follows

$$\dot{v} = M^{-1} (\sigma \tau_a + \bar{\tau}(t)) + \bar{f}(v) + \bar{w}(t). \quad (26)$$

The uncertain nonlinear term  $\bar{f}(v) = [\bar{f}_u(v), \bar{f}_v(v), \bar{f}_r(v)]^T$  can be estimated by some intelligent approximators, such as the following RBF network containing  $m_i$  neurons in the hidden layer

$$\bar{f}_i(v) = W_i^T \varphi_i(\zeta_i) + \varepsilon_i, \quad i = u, v, r \quad (27)$$

where  $W_i \in \mathbb{R}^{m_i}$  is the weight vector satisfying  $\|W_i\| \leq W_i^*$  with  $W_i^* \in \mathbb{R}^+$  being the upper bound,  $\varphi_i(\zeta_i) \in \mathbb{R}^{m_i}$  is the output vector of the hidden layer from the radial basis activation function,  $\zeta_i \in \Omega_{\zeta_i}$  is the input of the RBF network with  $\Omega_{\zeta_i}$  being a compact set, and  $\varepsilon_i \in \mathbb{R}$

is the approximation error satisfying  $|\varepsilon_i| \leq \varepsilon_i^*$  with  $\varepsilon_i^* \in \mathbb{R}^+$  being the upper bound.

According to the system structure, a neural predictor associated with (26) is constructed as follows

$$\dot{\hat{v}} = M^{-1} \hat{\sigma} \tau_a + \hat{w}_{\text{tot}} + \hat{f} - \kappa(\hat{v} - v) \quad (28)$$

where  $\hat{v} \in \mathbb{R}^3$  denotes an estimation of  $v$ ,  $\kappa = \text{diag}\{\kappa_u, \kappa_v, \kappa_r\}$  with  $\kappa_u, \kappa_v, \kappa_r \in \mathbb{R}^+$  being a diagonal gain matrix,  $\hat{f} = [\hat{W}_u^T \varphi_u(\zeta_u), \hat{W}_v^T \varphi_v(\zeta_v), \hat{W}_r^T \varphi_r(\zeta_r)]^T$  with  $\hat{W}_i$  being an estimation of  $W_i$ ,  $\hat{\sigma} = \text{diag}\{\hat{\sigma}_u, \hat{\sigma}_v, \hat{\sigma}_r\} \in \mathbb{R}^{3 \times 3}$  denotes an estimation of  $\sigma$ , and  $\hat{w}_{\text{tot}}$  is to be designed in the next step.

Then, an update law of  $\hat{W}_i$  can be designed for adaptive tuning as follows

$$\begin{cases} \dot{\hat{W}}_u = -\rho_u (\varphi_u(\zeta_u) \hat{u} + c_u \hat{W}_u) \\ \dot{\hat{W}}_v = -\rho_v (\varphi_v(\zeta_v) \hat{v} + c_v \hat{W}_v) \\ \dot{\hat{W}}_r = -\rho_r (\varphi_r(\zeta_r) \hat{r} + c_r \hat{W}_r) \end{cases} \quad (29)$$

where  $\rho_u, \rho_v, \rho_r \in \mathbb{R}^+$  are adaptation gains,  $c_u, c_v, c_r \in \mathbb{R}^+$  are tuning parameters, and  $\hat{u}, \hat{v}, \hat{r}$  satisfy  $\hat{v} = [\hat{u}, \hat{v}, \hat{r}]^T$  with  $\hat{v} = \hat{v} - v$ .

We can observe from (26) that there exists the unknown fault coefficient, which can be estimated by using some adaptation structures. An update law of  $\hat{\sigma}_i$  can be designed based on a concurrent learning approach as follows Chowdhary et al. (2013), Zhang et al. (2021) and Liu et al. (2021)

$$\begin{cases} \dot{\hat{\sigma}}_u = -\gamma_u \left[ \frac{\tau_{a,u} \hat{u}}{m_u} + d_u \sum_{l=1}^{N_u} \frac{\tau_{a,u}(l)}{m_u} \left( \frac{\hat{\sigma}_u(l) \tau_{a,u}(l)}{m_u} - \hat{u}(l) \right) \right] \\ \dot{\hat{\sigma}}_v = -\gamma_v \left[ \frac{\tau_{a,v} \hat{v}}{m_v} + d_v \sum_{l=1}^{N_v} \frac{\tau_{a,v}(l)}{m_v} \left( \frac{\hat{\sigma}_v(l) \tau_{a,v}(l)}{m_v} - \hat{v}(l) \right) \right] \\ \dot{\hat{\sigma}}_r = -\gamma_r \left[ \frac{\tau_{a,r} \hat{r}}{m_r} + d_r \sum_{l=1}^{N_r} \frac{\tau_{a,r}(l)}{m_r} \left( \frac{\hat{\sigma}_r(l) \tau_{a,r}(l)}{m_r} - \hat{r}(l) \right) \right] \end{cases} \quad (30)$$

where  $\gamma_u, \gamma_v, \gamma_r \in \mathbb{R}^+$  are adaptation gains,  $d_u, d_v, d_r \in \mathbb{R}^+$  are tuning parameters,  $N_u, N_v, N_r$  are the number of recorded data,  $\hat{\sigma}_u(l), \hat{\sigma}_v(l), \hat{\sigma}_r(l), \tau_{a,u}(l), \tau_{a,v}(l), \tau_{a,r}(l), \hat{u}(l), \hat{v}(l),$  and  $\hat{r}(l)$  are the  $l$ th recorded data.

**Step 2.** Kinetic control is considered in this step. At first, define a kinetic tracking error  $z_2 = \hat{v} - v_a$ . The dynamics of  $z_2$  is taken along (4) as follows

$$\dot{z}_2 = M^{-1} (\sigma \tau_a + \tilde{\tau}(t)) + \tilde{f}(v) + \tilde{w}(t) - v_a^d \quad (31)$$

The ocean disturbance  $\tilde{w}(t)$  is harmful to the ASV, which is similar to the unknown actuator bias  $\tilde{\tau}(t)$ .  $\tilde{w}(t)$  and  $\tilde{\tau}(t)$  are combined to degrade path maneuvering, and thus they are competing with the actual control input  $\tau_a$ . Therefore, the total disturbance is defined as  $w_{\text{tot}} = M^{-1} \tilde{\tau} + \tilde{w}$  and can be regarded as a player in the game. This competition can be considered as a two-player noncooperative game, in which  $\tau_a$  and  $w_{\text{tot}}$  are two players. Illustration of noncooperative game between kinetic control and total disturbance is shown in Fig. 3. Then, the dynamics of  $z_2$  is rewritten as follows

$$\dot{z}_2 = M^{-1} \sigma \tau_a + w_{\text{tot}} + \tilde{f}(v) - v_a^d. \quad (32)$$

Construct the following convex payoff function to describe this game as follows

$$J_v(z_2, \tau, \tau_d) = \int_0^\infty (z_2^T Q_v z_2 + \tau_a^T Q_a \tau_a - \lambda_v w_{\text{tot}}^T Q_w w_{\text{tot}}) dt \quad (33)$$

where  $Q_v \in \mathbb{R}^{3 \times 3}, Q_a \in \mathbb{R}^{3 \times 3}, Q_w \in \mathbb{R}^{3 \times 3}$  are given positive-definite diagonal matrices and  $\lambda_v \in \mathbb{R}^+$  denotes a coefficient.

In this game, we will try to find an optimal control input  $\tau_a$  to cover the worst total disturbance  $w_{\text{tot}}$  as far as possible. The mathematics process can be expressed as follows

$$J_v^*(z_2) = \min_{\tau_a} \max_{w_{\text{tot}}} J(z_2, \tau_a, w_{\text{tot}}). \quad (34)$$

Because the payoff function (33) is convex, there exists a Nash equilibrium  $(\tau_a^*, w_{\text{tot}}^*)$  in this game, such that the following inequality is achieved

$$J_v(z_2, \tau_a^*, w_{\text{tot}}^*) \leq J_v(z_2, \tau_a, w_{\text{tot}}^*) \leq J_v(z_2, \tau_a, w_{\text{tot}}) \quad (35)$$

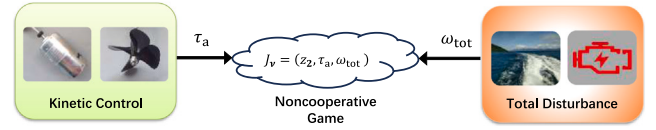


Fig. 3. Illustration of noncooperative game between kinetics control and total disturbance.

Then, the Hamiltonian function associated with (33) is expressed as follows

$$\begin{aligned} H_v(z_2, \nabla J_v(z_2), \tau_a, \tau_d) = & z_2^T Q_v z_2 + \tau_a^T Q_a \tau_a - \lambda_v w_{\text{tot}}^T Q_w w_{\text{tot}} \\ & + \nabla J_v^T(z_2) (M^{-1} \sigma \tau_a + w_{\text{tot}} \\ & + \tilde{f}(v) - v_a^d). \end{aligned} \quad (36)$$

The HJI function associated with (33) is obtained as below

$$0 = \min_{\tau_a} \max_{w_{\text{tot}}} J_v(z_2, \tau_a, w_{\text{tot}}). \quad (37)$$

Taking the partial derivative of the above HJI function, we can obtain the following two conditions

$$\frac{\partial H_v}{\partial \tau_a} = 0, \quad \frac{\partial H_v}{\partial w_{\text{tot}}} = 0. \quad (38)$$

Then, the optimal kinetic control law  $\tau_a^*$  and the worst total disturbance  $w_{\text{tot}}^*$  can be obtained along (36) as follows

$$\tau_a^* = -\frac{1}{2} Q_a^{-1} M^{-1} \sigma \nabla J_v^*(z_2) \quad (39)$$

$$w_{\text{tot}}^* = \frac{1}{2\lambda_v} Q_w^{-1} \nabla J_v^*(z_2). \quad (40)$$

Similar to the previous subsection, an adaptive dynamic programming policy can be used to solve the HJI function (36). A critic neural network consisting of  $p_v$  neurons can be used to identify  $J_v^*(z_2)$  as follows

$$J_v^*(z_2) = W_v^T \sigma_v(\zeta_v) + \varepsilon_v \quad (41)$$

where  $W_v \in \mathbb{R}^{p_v}$  is the weight vector of critic neural network satisfying  $\|W_v\| \leq W_v^*$  with  $W_v^* \in \mathbb{R}^+$  being the upper bound,  $\sigma_v(\zeta_v) \in \mathbb{R}^{p_v}$  is the output vector of the hidden layer with  $\zeta_v$  being the input, and  $\varepsilon_v \in \mathbb{R}$  is the approximation error satisfying  $|\varepsilon_v| \leq \varepsilon_v^*$  with  $\varepsilon_v^* \in \mathbb{R}^+$  being the upper bound.

Then,  $\nabla J_v^*(z_2)$  is expressed by the following form

$$\nabla J_v^*(z_2) = \nabla \sigma_v^T(\zeta_v) W_v + \nabla \varepsilon_v \quad (42)$$

where  $\nabla \sigma_v(\zeta_v) = \partial \sigma_v(\zeta_v) / \partial z_2 \in \mathbb{R}^{p_v \times 3}$  and  $\nabla \varepsilon_v = \partial \varepsilon_v / \partial z_2 \in \mathbb{R}^3$ . Substituting (42) into (39) and (40), we have

$$\tau_a^* = -\frac{1}{2} Q_a^{-1} M^{-1} \sigma (\nabla \sigma_v^T(\zeta_v) W_v + \nabla \varepsilon_v) \quad (43)$$

$$w_{\text{tot}}^* = \frac{1}{2\lambda_v} Q_w^{-1} (\nabla \sigma_v^T(\zeta_v) W_v + \nabla \varepsilon_v). \quad (44)$$

Substituting (43) and (44) into (36), the following HJI approximation error is obtained

$$\begin{aligned} \delta_v = & z_2^T Q_v z_2 + W_v^T \nabla \sigma_v(\zeta_v) (\hat{f} - v_a^d) \\ & - \frac{1}{4} W_v^T \nabla \sigma_v(\zeta_v) \sigma M^{-1} Q_a^{-1} M^{-1} \sigma \nabla \sigma_v^T(\zeta_v) W_v \\ & + \frac{1}{4\lambda_v} W_v^T \nabla \sigma_v(\zeta_v) Q_w^{-1} \nabla \sigma_v^T(\zeta_v) W_v. \end{aligned} \quad (45)$$

where  $\delta_v$  can be expressed by  $\delta_v = \delta_{\hat{u}} + \delta_{\hat{v}} + \delta_r + \delta_w$  and  $|\delta_l| \leq \delta_l^*$  with  $l = \hat{u}, \hat{v}, r, w$  and  $\delta_l^* \in \mathbb{R}^+$  being a residual error (Ren et al., 2022; Ma et al., 2023).

Because the real value of  $W_v$  cannot be obtained, two estimations  $\hat{\tau}_a = [\hat{\tau}_{a,\bar{u}}, \hat{\tau}_{a,\bar{v}}, \hat{\tau}_{a,r}]^T$  and  $\hat{w}_{\text{tot}}$  can be constructed as follows

$$\begin{cases} \hat{\tau}_{a,\bar{u}} = -\frac{1}{2q_{a,\bar{u}}} R_{\bar{u}}^T (\nabla \sigma_v^T(\zeta_v) \hat{W}_{a,\bar{u}}) \\ \hat{\tau}_{a,\bar{v}} = -\frac{1}{2q_{a,\bar{v}}} R_{\bar{v}}^T (\nabla \sigma_v^T(\zeta_v) \hat{W}_{a,\bar{v}}) \\ \hat{\tau}_{a,r} = -\frac{1}{2q_{a,r}} R_r^T (\nabla \sigma_v^T(\zeta_v) \hat{W}_{a,r}) \end{cases} \quad (46)$$

$$\hat{w}_{\text{tot}} = \frac{1}{2\lambda_v} Q_w^{-1} (\nabla \sigma_v^T(\zeta_v) \hat{W}_v) \quad (47)$$

where  $[R_{\bar{u}}, R_{\bar{v}}, R_r] = M^{-1}$ ,  $\text{diag}\{q_{a,\bar{u}}, q_{a,\bar{v}}, q_{a,r}\} = Q_a$ ,  $\hat{W}_{a,\bar{u}}$  is the estimation of  $\sigma_u W_v$ ,  $\hat{W}_{a,\bar{v}}$  is the estimation of  $\sigma_v W_v$ ,  $\hat{W}_{a,r}$  is the estimation of  $\sigma_r W_v$ , and  $\hat{W}_v$  is the estimation of  $\sigma_r W_v$ .  $\hat{\tau}_a$  is sent to the actuator of ASV to replace  $\tau_a$  such that  $\hat{\tau}_a = \tau_a$ .

An approximated Hamilton function is constructed as

$$\begin{aligned} e_v &= z_2^T Q_v z_2 + \hat{W}_v^T \nabla \sigma_v(\zeta_v) (\hat{f} - v^d) \\ &- \sum_{i=\bar{u}}^{\bar{v},r} \frac{1}{4q_{a,i}} \hat{W}_{a,i}^T \nabla \sigma_v(\zeta_v) R_i^T R_i \nabla \sigma_v^T(\zeta_v) \hat{W}_{a,i} \\ &+ \frac{1}{4\lambda_v} \hat{W}_v^T \nabla \sigma_v(\zeta_v) Q_w^{-1} \nabla \sigma_v^T(\zeta_v) \hat{W}_v. \end{aligned} \quad (48)$$

$e_v$  can be further divided into two parts  $e_v = \sum_{i=\bar{u}}^{\bar{v},r} e_{a,i} + e_{\text{tot}}$ , where  $e_{a,i}$  is the sub-term in  $e_v$  containing  $\hat{W}_{a,i}$  and  $e_{\text{tot}}$  is the sub-term in  $e_v$  containing  $\hat{W}_v$ . Then, define two squared residual errors  $E_{a,i}$  and  $E_{\text{tot}}$  as follows

$$E_{a,i} = \frac{1}{2} e_{a,i}^2 \quad (49)$$

$$E_{\text{tot}} = \frac{1}{2} e_{\text{tot}}^2. \quad (50)$$

The update law of  $\hat{W}_{a,i}$  and  $\hat{W}_v$  can be constructed as follows

$$\begin{cases} \dot{\hat{W}}_{a,i} = -\rho_{a,i} \left[ \frac{\varphi_{a,i}}{(1+\varphi_{a,i}^T \varphi_{a,i})^2} e_{a,i} - \frac{\varphi_{a,i}}{4(1+\varphi_{a,i}^T \varphi_{a,i})^2} \hat{W}_{a,i}^T D_{a,i} \hat{W}_{a,i} \right. \\ \quad \left. - B_{i,1} \hat{W}_{a,i} \right], \quad i = \bar{u}, \bar{v}, r \\ \dot{\hat{W}}_v = -\rho_w \left[ \frac{\varphi_w}{(1+\varphi_w^T \varphi_w)^2} e_{\text{tot}} + \frac{\varphi_w}{4\theta(1+\varphi_w^T \varphi_w)^2} \hat{W}_v^T D_d \hat{W}_v \right. \\ \quad \left. - B_{w,1} \hat{W}_v \right] \end{cases} \quad (51)$$

where  $\rho_{a,i}, \rho_w \in \mathbb{R}^+$  are adaptation gains,  $\varphi_{a,i} = -(1/2)D_{a,i} \hat{W}_{a,i}$ ,  $D_{a,i} = \nabla \sigma_v(\zeta_v) R_i^T q_i^{-1} R_i \nabla \sigma_v^T(\zeta_v)$ ,  $\varphi_w = \nabla \sigma_v(\zeta_v) (\hat{f} - v^d) + (1/2\lambda_v) D_w \hat{W}_v$ ,  $D_w = \nabla \sigma_v(\zeta_v) Q_w^{-1} \nabla \sigma_v^T(\zeta_v)$ ,  $B_{i,1}, B_{w,1} \in \mathbb{R}^{\rho_v \times \rho_v}$  are two tuning parameter matrices.

#### 4. Main results

The closed-loop system resulting from the proposed path maneuvering control method is more complicated than the one resulting from the conventional path maneuvering control method such as Skjetne et al. (2004, 2005), Zhang et al. (2017, 2022), Liu et al. (2020), Lv et al. (2023, 2022), Peng et al. (2018, 2020), Gu et al. (2021) and Zhang et al. (2021, 2023) due to the ADP strategy. Nevertheless, it is still possible to establish that the closed-loop system still retain the uniform boundedness property via the analysis of the input-to-state stability. To this end, we conclude the following theorem.

**Theorem 1.** Consider the ASV governed by (4). When the robust adaptive fault-tolerant path maneuvering controller is chosen as kinematic law (8), second-order nonlinear tracking differentiator (9), optimal path update law (22), neural predictor (28) and (29), kinetic control law (46), expected worst total disturbance (48), and update laws for the critic neural network (25) and (51) under the noncooperative game mechanisms (11) and (33), the total closed-loop system is input-to-state stable.

**Proof.** The total closed-loop system can be divided into three subsystems, including an estimation subsystem, a kinetics subsystem, and a kinematics subsystem. At first, we consider the estimation subsystem. Define  $\tilde{v} = \hat{v} - v$ ,  $\tilde{W}_i = \hat{W}_i - W_i$ , and  $\tilde{\sigma}_i = \hat{\sigma}_i - \sigma_i$ , and the dynamics of  $\tilde{v}$ ,  $\tilde{W}_i$ , and  $\tilde{\sigma}_i$  is given as

$$\Sigma_e : \begin{cases} \dot{\tilde{v}} = -\kappa \tilde{v} + M^{-1} \tilde{\sigma} \tau_a + \hat{w}_{\text{tot}} + \tilde{f} - \varepsilon \\ \dot{\tilde{W}}_{\bar{u}} = -\rho_u (\varphi_u(\zeta_u) \tilde{u} + c_u \tilde{W}_{\bar{u}}) \\ \dot{\tilde{W}}_{\bar{v}} = -\rho_v (\varphi_v(\zeta_v) \tilde{v} + c_v \tilde{W}_{\bar{v}}) \\ \dot{\tilde{W}}_r = -\rho_r (\varphi_r(\zeta_r) \tilde{r} + c_r \tilde{W}_r) \\ \dot{\tilde{\sigma}}_u = -\gamma_u \left[ \frac{\tau_{a,\bar{u}} \tilde{u}}{m_u} + d_u \sum_{l=1}^{N_u} \frac{\tau_{a,\bar{u}}(l)}{m_u} \left( \frac{\hat{\sigma}_u(l) \tau_{a,\bar{u}}(l)}{m_u} - \hat{u}(l) \right) \right] \\ \dot{\tilde{\sigma}}_v = -\gamma_v \left[ \frac{\tau_{a,\bar{v}} \tilde{v}}{m_v} + d_v \sum_{l=1}^{N_v} \frac{\tau_{a,\bar{v}}(l)}{m_v} \left( \frac{\hat{\sigma}_v(l) \tau_{a,\bar{v}}(l)}{m_v} - \hat{v}(l) \right) \right] \\ \dot{\tilde{\sigma}}_r = -\gamma_r \left[ \frac{\tau_{a,r} \tilde{r}}{m_r} + d_r \sum_{l=1}^{N_r} \frac{\tau_{a,r}(l)}{m_r} \left( \frac{\hat{\sigma}_r(l) \tau_{a,r}(l)}{m_r} - \hat{r}(l) \right) \right] \end{cases} \quad (52)$$

where  $\hat{w}_{\text{tot}} = \hat{w}_{\text{tot}} - w_{\text{tot}}$ ,  $\tilde{f} = [\tilde{W}_{\bar{u}}^T \varphi_u(\zeta_u), \tilde{W}_{\bar{v}}^T \varphi_v(\zeta_v), \tilde{W}_r^T \varphi_r(\zeta_r)]^T$ ,  $\varepsilon = [\varepsilon_u, \varepsilon_v, \varepsilon_r]^T$ . The states of the estimation subsystem  $\Sigma_e$  consist of  $\tilde{v}$ ,  $\tilde{W}_i$ , and  $\tilde{\sigma}_i$ . The inputs of the estimation subsystem  $\Sigma_e$  consist of  $\varepsilon$ ,  $W_i$ , and  $\sigma_i$ . Choose

$$V_e = \frac{1}{2} \tilde{v}^T \tilde{v} + \sum_{i=\bar{u}}^{\bar{v},r} \frac{1}{2\gamma_i} \tilde{W}_i^T \tilde{W}_i + \sum_{i=\bar{u}}^{\bar{v},r} \frac{1}{2\gamma_i} \tilde{\sigma}_i^2 \quad (53)$$

as a candidate Lyapunov function for the subsystem  $\Sigma_e$ .

Taking the derivative of  $V_e$  along (52), we have

$$\begin{aligned} \dot{V}_e &= -\tilde{v}^T \kappa \tilde{v} + \tilde{v}^T \hat{w}_{\text{tot}} - \tilde{v}^T \varepsilon - \sum_{i=\bar{u}}^{\bar{v},r} c_i \tilde{W}_i^T \tilde{W}_i - \sum_{i=\bar{u}}^{\bar{v},r} d_i \tilde{\sigma}_i \tilde{\sigma}_i \\ &= -\tilde{v}^T \kappa \tilde{v} + \tilde{v}^T \hat{w}_{\text{tot}} - \tilde{v}^T \varepsilon - \sum_{i=\bar{u}}^{\bar{v},r} c_i \tilde{W}_i^T (\tilde{W}_i + W_i) \\ &\quad - \sum_{i=\bar{u}}^{\bar{v},r} d_i \tilde{\sigma}_i \left[ \sum_{l=1}^{N_i} \frac{\tau_{a,i}(l)}{m_i} \left( \frac{\tilde{\sigma}_i(l) \tau_{a,i}(l)}{m_i} \right) \right]. \end{aligned} \quad (54)$$

Define  $\tilde{W} = [\tilde{W}_{\bar{u}}^T, \tilde{W}_{\bar{v}}^T, \tilde{W}_r^T]^T$  and  $\tilde{\sigma} = [\tilde{\sigma}_u, \tilde{\sigma}_v, \tilde{\sigma}_r]^T$ , (54) can be further put into

$$\dot{V}_e \leq -\lambda_{\min}(\kappa) \|\tilde{v}\|^2 + \|\tilde{v}\| \|\hat{w}_{\text{tot}}\| + \|\tilde{v}\| \|\varepsilon\| - \lambda_{\min}(c_e) \|\tilde{W}\|^2 + \lambda_{\max}(c_e) \|\tilde{W}\| \|W\| - \lambda_{\min}(d_e) p_e \|\tilde{\sigma}\|^2 \quad (55)$$

where  $W = [W_{\bar{u}}^T, W_{\bar{v}}^T, W_r^T]^T$ ,  $\sigma = [\sigma_u, \sigma_v, \sigma_r]^T$ ,  $c_e = \text{diag}\{c_u, c_v, c_r\}$ ,  $d_e = \text{diag}\{d_u, d_v, d_r\}$ , and  $p_e = \min(N_i) \min(\tau_i^2(l)/\max(m_i^2))$ .

Then, it follows that

$$\dot{V}_e \leq -q_e \|E_e\|^2 + \|E_e\| \|U_e\| \quad (56)$$

where  $q_e = \min\{\lambda_{\min}(\kappa), \lambda_{\min}(c_e), \lambda_{\min}(d_e) p_e\}$ ,  $E_e = [\|\tilde{v}\|, \|\tilde{W}\|, \|\tilde{\sigma}\|]^T$ , and  $U_e = [\|\hat{w}_{\text{tot}}\|, \|\varepsilon\|, \lambda_{\max}(c_e) \|W\|]^T$ .

Since  $\|E_e\| \geq 2\|U_e\|/q_e$  makes  $\dot{V}_e \leq -q_e \|E_e\|^2/2$ , the estimation subsystem  $\Sigma_e$  governed by (52) is input-to-state stable based on Definition 4.4 and Theorem 4.6 in Khalil (2015). Then, we can write the solution of (56)  $\|E_e\|(t)$  for all  $t > t_0$  as follows

$$\|E_e(t)\| \leq -e^{\kappa(t-t_0)} E_e(t_0) + g_e \left( \sup_{t_0 < \tau < t} \|U_e(\tau)\| \right) \quad (57)$$

Letting  $V_e^* = (1/2)(\tilde{v}^T \tilde{v} + \sum_{i=\bar{u}}^{\bar{v},r} \tilde{W}_i^T \tilde{W}_i + \sum_{i=\bar{u}}^{\bar{v},r} \tilde{\sigma}_i^2)$  and  $\Phi_e = \text{diag}\{1, 1/\rho_u, 1/\rho_v, 1/\rho_r, 1/\gamma_u, 1/\gamma_v, 1/\gamma_r\}$ ,  $V_e$  satisfies the following form

$$\lambda_{\min}(\Phi_e) V_e^* \leq V_e \leq \lambda_{\max}(\Phi_e) V_e^*.$$

Define  $h_1(\tilde{v}, \tilde{W}_i, \tilde{\sigma}_i) = \lambda_{\min}(\Phi_e) V_e^*$  and  $h_2(\tilde{v}, \tilde{W}_i, \tilde{\sigma}_i) = \lambda_{\max}(\Phi_e) V_e^*$ . By using Theorem 4.6 in Khalil (2015), we have

$$\begin{aligned} g_e \left( \sup_{t_0 < \tau < t} \|U_e\|(\tau) \right) &= \frac{2}{q_e} h_1^{-1} \circ h_2 \left( \sup_{t_0 < \tau < t} \|U_e(\tau)\| \right) \\ &= \frac{2\sqrt{\lambda_{\min}(\Phi_e)}}{q_e \sqrt{\lambda_{\max}(\Phi_e)}} \sup_{t_0 < \tau < t} \|U_e(\tau)\|. \end{aligned} \quad (58)$$

Because  $\|U_e\| \leq \|\hat{w}_{\text{tot}}\| + \|\varepsilon\| + \lambda_{\max}(c_e)\|W\|$ , (57) can be further put into the following form based on (58)

$$\|E_e(t)\| \leq \beta_e(E_e(t_0), t - t_0) + g_{\hat{w}}(\|\hat{w}_{\text{tot}}\|) + g_\varepsilon(\|\varepsilon\|) + g_W(\|W\|) \quad (59)$$

where  $\beta_e(\cdot)$  is a class  $\mathcal{KL}$  functions satisfying  $\beta_e(s) = -e^{\kappa(t-t_0)}s$ , and  $g_{\hat{w}}(\cdot)$ ,  $g_\varepsilon(\cdot)$ ,  $g_W(\cdot)$  are class  $\mathcal{K}$  function satisfying  $g_{\hat{w}}(s) = g_\varepsilon(s) = 2\sqrt{\lambda_{\min}(\Phi_e)s}/\sqrt{\lambda_{\max}(\Phi_e)q_e}$ ,  $g_W(s) = 2\sqrt{\lambda_{\min}(\Phi_e)\lambda_{\max}(c_e)s}/\sqrt{\lambda_{\max}(\Phi_e)q_e}$ .

Then, we consider the kinematics and path update subsystem. Letting  $\bar{W}_d = \hat{W}_d - W_d$ , the dynamics of  $\bar{W}_d$  is expressed by the following form

$$\dot{\bar{W}}_d = -\rho_d \left( \bar{\vartheta}_d \bar{\vartheta}_d^T \bar{W}_d - \bar{\vartheta}_d \frac{\delta_d}{\chi_d} \right) \quad (60)$$

where  $\bar{\vartheta}_d = \vartheta_d/(1 + \vartheta_d^T \vartheta_d)$  and  $\chi_d = 1 + \vartheta_d^T \vartheta_d$ .

The states of the kinematics and path update subsystem consist of  $z_1$ ,  $z_d$ , and  $\bar{W}_d$ . The error dynamics of this subsystem is expressed by the following form

$$\Sigma_a : \begin{cases} \dot{z}_1 = -K_1 z_1 + t_1 + z_2 \\ \dot{z}_d = \omega - v_s \\ \dot{\bar{W}}_d = -\rho_d \left( \bar{\vartheta}_d \bar{\vartheta}_d^T \bar{W}_d - \bar{\vartheta}_d \frac{\delta_d}{\chi_d} \right) \end{cases} \quad (61)$$

where  $t_1 = v_a - \alpha$  denotes the filter error.

Choose

$$V_a = \frac{1}{2} \bar{z}_1^T \bar{z}_1 + \frac{1}{2\rho_d} \bar{W}_d^T \bar{W}_d + J_d(z_d) \quad (62)$$

as a candidate Lyapunov function for the subsystem  $\Sigma_a$ .

Taking the derivative of  $V_a$  along (61), we have

$$\dot{V}_a = -z_1^T K_1 z_1 + \bar{z}_1^T t_1 + \bar{z}_1^T z_2 - \bar{W}_d^T \left( \bar{\vartheta}_d \bar{\vartheta}_d^T \bar{W}_d - \bar{\vartheta}_d \frac{\delta_d}{\chi_d} \right) + J_d(z_d). \quad (63)$$

According to Lemma 1 in Ma et al. (2023), we can obtain

$$\begin{aligned} J_d(z_d) &= \nabla J_d(z_d)(\omega - v_s) \\ &\leq -\frac{\nabla J_d^2(z_d)}{4\Pi_d} - \frac{-c\| -K_1 z_1 - k_d \eta_r^\theta(\theta) z_d\|^2}{\Pi_d}. \end{aligned} \quad (64)$$

Define  $Z_1 = [\|z_1\|, \|z_d\|]^T$ , and then (64) can be further put into

$$\begin{aligned} \dot{V}_a &\leq -\frac{\lambda_{\min}(Q_d)}{\Pi_d} \|Z_1\|^2 - \|\bar{\vartheta}_d\|^2 \|\bar{W}_d\| + \|z_1\|(\|t_1\| + \|z_2\|) \\ &\quad + \left\| \frac{\bar{\vartheta}_d}{\chi_d} \right\| \|\bar{W}_d\| |\delta_d| \end{aligned} \quad (65)$$

where  $Q_d = \begin{bmatrix} (\Pi_d + c_d)\lambda_{\min}(K_1) & -0.5(\lambda_{\max}(K_1)k_d)\|\eta_r^\theta(\theta)\| \\ -0.5(\lambda_{\max}(K_1)k_d)\|\eta_r^\theta(\theta)\| & c_d k_d \|\eta_r^\theta(\theta)\| \end{bmatrix}$ .

Define  $E_a = [\|Z_1\|, \|\bar{W}_d\|]^T$ . It follows that

$$\dot{V}_a \leq -q_a \|E_a\|^2 + \|E_a\| \left( \|t_1\| + \|z_2\| + \left\| \frac{\bar{\vartheta}_d}{\chi_d} \right\| |\delta_d| \right) \quad (66)$$

where  $q_a = \min\{\lambda_{\min}(Q_d)/\Pi_d, \|\bar{\vartheta}_d\|^2\}$ .

Since  $\|E_a\| \geq 2(\|t_1\| + \|z_2\| + \|\bar{\vartheta}_d/\chi_d\| |\delta_d|)/q_a$  makes  $\dot{V}_a \leq -q_a \|E_a\|^2/2$ , the subsystem  $\Sigma_a$  governed by (61) is input-to-state stable based on Definition 4.4 and Theorem 4.6 in Khalil (2015). Then, we can obtain the solution of (66)  $\|E_a\|(t)$  for all  $t > t_0$  as follows

$$\|E_a(t)\| \leq -e^{\kappa(t-t_0)} E_a(t_0) + g_a \left( \sup_{t_0 < \tau < t} U_a(\tau) \right) \quad (67)$$

where  $U_a(\tau) = \|t_1(\tau)\| + \|z_2(\tau)\| + \|\bar{\vartheta}_d/\chi_d\| |\delta_d(\tau)|$ .

Letting  $V_a^* = (1/2)(\bar{z}_1^T \bar{z}_1 + \bar{W}_d^T \bar{W}_d + J_d(z_d))$  and  $\Phi_d = \text{diag}\{1, 1/\rho_d, 2\}$ ,  $V_d$  satisfies the following form

$$\lambda_{\min}(\Phi_a)V_a^* \leq V_a \leq \lambda_{\max}(\Phi_a)V_a^*.$$

Define  $h_1(Z_1, \bar{W}_d) = \lambda_{\min}(\Phi_d)V_d^*$  and  $h_2(Z_1, \bar{W}_d) = \lambda_{\max}(\Phi_d)V_d^*$ . By using Theorem 4.6 in Khalil (2015), we have

$$\begin{aligned} g_a \left( \sup_{t_0 < \tau < t} U_d(\tau) \right) &= \frac{2}{q_a} h_1^{-1} \circ h_2 \left( \sup_{t_0 < \tau < t} U_a(\tau) \right) \\ &= \frac{2\sqrt{\lambda_{\min}(\Phi_d)}}{q_a \sqrt{\lambda_{\max}(\Phi_d)}} \sup_{t_0 < \tau < t} U_a(\tau). \end{aligned} \quad (68)$$

Then, by using (68), (67) can be further put into

$$\|E_a(t)\| \leq \beta_a(E_a(t_0), t - t_0) + g_{t_1}(\|t_1\|) + g_{z_2}(\|z_2\|) + g_{\delta_d}(|\delta_d|) \quad (69)$$

where  $\beta_a(\cdot)$  is a class  $\mathcal{KL}$  function satisfying  $\beta_a(s) = -e^{\kappa(t-t_0)}s$ , and  $g_{t_1}(\cdot)$ ,  $g_{z_2}(\cdot)$ , and  $g_{\delta_d}(\cdot)$  are class  $\mathcal{K}$  functions satisfying  $g_{t_1}(s) = g_{z_2}(s) = 2\sqrt{\lambda_{\min}(\Phi_a)s}/\sqrt{\lambda_{\max}(\Phi_a)q_a}$ , and  $g_{\delta_d}(s) = 2\sqrt{\lambda_{\min}(\Phi_a)}\|\bar{\vartheta}_d\|s/\sqrt{\lambda_{\max}(\Phi_a)}\chi_d|q_a$ .

Then, we consider the kinetics. The states of the kinetic subsystem include  $\hat{z}_2$ ,  $\bar{W}_{a,i} = W_{a,i} - \hat{W}_{a,i}$ , and  $\bar{W}_v = W_v - \hat{W}_v$ . The dynamics of  $\bar{W}_{a,i}$  and  $\bar{W}_v$  is given by

$$\begin{aligned} \dot{\bar{W}}_{a,i} &= -\hat{W}_{a,i} \\ &= -\rho_{a,i}(\varphi_{a,i}\varphi_{a,i}^T \bar{W}_{a,i} - B_{a,1} \hat{W}_{a,i} \\ &\quad - \frac{\varphi_{a,i}}{(1 + \varphi_{a,i}^T \varphi_{a,i})^2} \left( \frac{1}{4} \bar{W}_{a,i}^T D_{a,i} \bar{W}_{a,i} + \delta_i \right) \\ &\quad + \frac{\varphi_{a,i}}{4(1 + \varphi_{a,i}^T \varphi_{a,i})^2} \hat{W}_{a,i}^T D_{a,i} \hat{W}_{a,i}) \end{aligned} \quad (70)$$

$$\begin{aligned} \dot{\bar{W}}_v &= -\hat{W}_v \\ &= -\rho_v(\varphi_v \varphi_v^T \bar{W}_v - B_{w,1} \hat{W}_v \\ &\quad - \frac{\varphi_v}{(1 + \varphi_v^T \varphi_v)^2} \left( \frac{1}{4\lambda_v} \bar{W}_v^T D_w \bar{W}_v + \delta_w \right) \\ &\quad + \frac{\varphi_v}{4\lambda_v(1 + \varphi_v^T \varphi_v)^2} \hat{W}_v^T D_w \hat{W}_v). \end{aligned} \quad (71)$$

The dynamics of the kinetic subsystem can be expressed by the following form

$$\Sigma_v : \begin{cases} \dot{\hat{z}}_2 = M^{-1} \hat{\sigma} \tau_a + \hat{w}_{\text{tot}} + \hat{f} - \kappa \bar{v} - v_d^d \\ \dot{\bar{W}}_{a,i} = -\hat{W}_{a,i} \\ \dot{\bar{W}}_v = -\hat{W}_v \end{cases} \quad (72)$$

Choose

$$V_v = \sum_{i=\hat{u}}^{\bar{v},r} \frac{1}{2\rho_{a,i}} \bar{W}_{a,i}^T \bar{W}_{a,i} + \frac{1}{2\rho_v} \bar{W}_v^T \bar{W}_v + J_v(\hat{z}_2) \quad (73)$$

as a candidate Lyapunov function for the subsystem  $\Sigma_v$ .

Taking the derivative of  $V_v$  along (72), we have

$$\dot{V}_v = -\sum_{i=\hat{u}}^{\bar{v},r} \bar{W}_{a,i}^T \dot{\bar{W}}_{a,i} - \bar{W}_v^T \dot{\bar{W}}_v + J_v(\hat{z}_2). \quad (74)$$

According to Lemma 1 in Ma et al. (2023), we can obtain that

$$J_d(z_d) = -\nabla J_v^T(\hat{z}_2)G(\hat{z}_2)\nabla J_v(\hat{z}_2) \quad (75)$$

Then, it follows that

$$\begin{aligned} \dot{V}_v &\leq -\lambda_{\min}(Q_v)\|\hat{z}_2\|^2 - (\|\varphi_v\|^2 + \lambda_{\min}(B_w))\|\bar{W}_v\|^2 \\ &\quad - \sum_{i=\hat{u}}^{\bar{v},r} (\|\varphi_{a,i}\|^2 + \lambda_{\min}(B_{a,i}))\|\bar{W}_{a,i}\|^2 \\ &\quad + \sum_{i=\hat{u}}^{\bar{v},r} \|\bar{W}_{a,i}\| \left( \frac{1}{2} b_{a,i} \lambda_{\max}(D_{a,i}) \|\bar{W}_{a,i}\| \|W_{a,i}\| \right. \\ &\quad \left. + \lambda_{\max}(B_{a,i}) \|W_{a,i}\| + b_{a,i} \|\delta_i\| \right) \\ &\quad + \|\bar{W}_v\| \left( \frac{1}{2\lambda_v} b_v \lambda_{\max}(D_w) \|\bar{W}_v\| \|W_v\| \right. \\ &\quad \left. + \lambda_{\max}(B_v) \|W_v\| + b_v \|\delta_w\| \right) \end{aligned} \quad (76)$$

where  $b_{a,i} = \|\varphi_{a,i}\|/(1 + \varphi_{a,i}^T \varphi_{a,i})^2$  and  $b_v = \|\varphi_v\|/(1 + \varphi_v^T \varphi_v)^2$ .

Define  $E_v = [\|\hat{z}_2\|, \|\tilde{W}_{a,\bar{u}}\|, \|\tilde{W}_{a,\bar{v}}\|, \|\tilde{W}_{a,r}\|, \|\tilde{W}_v\|]^T$ , and one can further put into

$$\begin{aligned} \dot{V}_v \leq & -q_v \|E_v\|^2 + \|E_v\| \sum_{i=\bar{u}}^{\bar{v},r} (\lambda_{\max}(B_{a,i}) \|W_{a,i}\| + b_{a,i} \\ & \times \|\delta_i\|) + \|E_v\| (\lambda_{\max}(B_v) \|W_v\| + b_v \|\delta_w\|) \end{aligned} \quad (77)$$

where  $q_v = \min_{i=\bar{u},\bar{v},r} \{\lambda_{\min}(Q_v), (\|\varphi_v\|^2 + \lambda_{\min}(B_w) - b_v \lambda_{\max}(D_w) W_v^*/2\lambda_v), (\|\varphi_{a,i}\|^2 + \lambda_{\min}(B_{a,i}) - 0.5b_{a,i} \lambda_{\max}(D_{a,i}) W_{a,i}^*)\}$ . Appropriate parameters should be chosen to make  $q_v > 0$ .

Since  $\|E_v\| \geq 2(\sum_{i=\bar{u}}^{\bar{v},r} (\lambda_{\max}(B_{a,i}) \|W_{a,i}\| + b_{a,i} \|\delta_i\|) + (\lambda_{\max}(B_v) \|W_v\| + b_v \|\delta_w\|))/q_v$  makes  $\dot{V}_v \leq -q_v \|E_v\|^2/2$ , the subsystem  $\Sigma_v$  governed by (72) is input-to-state stable. Similar to subsystems  $\Sigma_e$  and  $\Sigma_a$ , letting  $\Phi_v = \text{diag}\{1, 1/\rho_{a,\bar{u}}, 1/\rho_{a,\bar{v}}, 1/\rho_{a,r}, 1/\rho_v\}$ ,  $\|E_v(t)\|$  satisfies

$$\begin{aligned} \|E_v(t)\| \leq & \beta_v (E_v(t_0), t - t_0) + \sum_{i=\bar{u}}^{\bar{v},r} (g_{W_{a,i}}(\|W_{a,i}\|) + g_{\delta_i}(\|\delta_i\|)) \\ & + g_{W_v}(\|W_v\|) + g_{\delta_w}(\|\delta_w\|) \end{aligned} \quad (78)$$

where  $\beta_v(\cdot)$  is a class  $\mathcal{KL}$  function, and  $g_{W_{a,i}}(\cdot)$ ,  $g_{\delta_i}(\cdot)$ ,  $g_{W_v}(\cdot)$ , and  $g_{\delta_w}(\cdot)$  are class  $\mathcal{K}$  functions satisfying  $g_{W_{a,i}}(s) = 2\sqrt{\lambda_{\min}(\Phi_v)} \lambda_{\max}(B_{a,i}) s / \sqrt{\lambda_{\max}(\Phi_v) q_v}$ ,  $g_{W_v}(s) = 2\sqrt{\lambda_{\min}(\Phi_v)} \lambda_{\max}(B_v) s / \sqrt{\lambda_{\max}(\Phi_v) q_v}$ ,  $g_{\delta_i}(s) = g_{\delta_w}(s) = 2b_v \sqrt{\lambda_{\min}(\Phi_v) s} / \sqrt{\lambda_{\max}(\Phi_v) q_v}$ .

At last, we consider the input-to-state stability property of the total closed-loop system. At first, we have  $z_2 = \tilde{v} - v_a = \hat{v} - v_a + \tilde{v} - \hat{v} = \hat{z}_2 - \tilde{v}$ . According to the property of class  $\mathcal{K}$  function, (69) can be further put into

$$\begin{aligned} \|E_a(t)\| \leq & \beta_a (E_a(t_0), t - t_0) + g_{t_1}(\|t_1\|) + g_{z_2}(\|\hat{z}_2 - \tilde{v}\|) \\ & + g_{\delta_d}(\|\delta_d\|) \\ \leq & \beta_a (E_a(t_0), t - t_0) + g_{t_1}(\|t_1\|) + g_{z_2}(\|\hat{z}_2\|) \\ & + g_{z_2}(\|\tilde{v}\|) + g_{\delta_d}(\|\delta_d\|). \end{aligned} \quad (79)$$

$\hat{z}_2$  and  $\tilde{v}$  can be considered as two inputs of the subsystem  $\Sigma_a$ . Because  $\tilde{v}$  is one of states of the subsystem  $\Sigma_e$  and  $\hat{z}_2$  is one of states of the subsystem  $\Sigma_v$ , the total closed-loop system is a cascade system based on Lemma C.4 in Krstic et al. (1995), which some states of subsystems  $\Sigma_e$  and  $\Sigma_v$  are connected with the subsystem  $\Sigma_a$ . Because  $\tilde{v} \in E_e$  and  $\hat{z}_2 \in E_v$ , (79) can be transformed into the following form eventually

$$\begin{aligned} \|E_a(t)\| \leq & \beta_a (E_a(t_0), t - t_0) + g_{t_1}(\|t_1\|) + g_{z_2} \circ [ \sum_{i=\bar{u}}^{\bar{v},r} (g_{W_{a,i}}(\|W_{a,i}\|) \\ & + g_{\delta_i}(\|\delta_i\|) + g_{W_v}(\|W_v\|) \\ & + g_{\delta_w}(\|\delta_w\|) ] + g_{z_2} \circ (g_{\tilde{v}}(\|\tilde{v}\|) + g_{\delta_d}(\|\delta_d\|)) \\ & + g_{\epsilon}(\|\epsilon\|) + g_W(\|W\|) + g_{\delta_d}(\|\delta_d\|). \end{aligned}$$

The proof is complete.

**Remark 2.** The noncooperative game can be regarded as an extension of optimization. If there is only one player, the noncooperative game can be viewed as the optimal control problem. For the noncooperative game (11), the path update scheme  $\omega$ , as one player, aims to reduce the payoff function  $J_d(\omega, z_d)$  as far as possible, but the kinematic control term  $\alpha$ , as another player, is independent because it is employed to achieve kinematic control task. If we only consider  $\omega$  as a single player,  $J_d(\omega, z_d)$  is the same as the optimal control problem. For the second game (33), the actual control input  $\tau_a$ , as one player, aims to achieve the kinetic control task as far as possible, but the total disturbance  $w_{\text{tot}}$ , as another player, aims to destroy the control task as far as possible. If we only consider  $\tau_a$  as a single player,  $J_v(z_2, \tau_a, w_{\text{tot}})$  is same to the optimal control problem.

**Remark 3.** Many algorithms for optimization problems can be employed to solve payoff functions of noncooperative games. Except for

ADP, there are other approaches to solve the payoff functions of noncooperative games, such as policy iteration, Hamilton analysis, and neurodynamic optimization.

## 5. Simulation example

We give a series of simulation results to show the effectiveness of the robust adaptive fault-tolerant path maneuvering control method. Internal parameters of the ASV considered herein can be referred to Fossen (2011). The simulation scenario is considered to occur in Siyuan Lake, Shanghai.

We let simulation parameters to be  $K_1 = \text{diag}\{0.2, 0.2, 0.2\}$ ,  $\gamma_a = 4$ ,  $\beta_{a,1} = 1$ ,  $\beta_{a,2} = 2$ ,  $c_d = 50$ ,  $k_d = 50$ ,  $\rho_d = 0.02$ ,  $\kappa = \text{diag}\{210, 210, 210\}$ ,  $\rho_u = \rho_v = \rho_r = 1000$ ,  $c_u = c_v = c_r = 0.00005$ ,  $\gamma_u = \gamma_v = 0.08$ ,  $\gamma_r = 0.003$ ,  $d_u = d_v = 0.008$ ,  $d_r = 0.00005$ ,  $N_\sigma = 500$ ;  $Q_v = \text{diag}\{0.2, 0.2, 0.2\}$ ,  $Q_a = \text{diag}\{0.01, 0.01, 0.01\}$ ,  $Q_w = \text{diag}\{0.01, 0.01, 0.01\}$ ,  $\rho_{a,u} = \rho_{a,v} = \rho_{a,r} = 0.03$ ,  $\rho_w = 0.001$ ,  $B_{a,u} = B_{a,v} = B_{a,r} = B_w = \text{diag}\{0.0002, 0.0002, 0.0002\}$ ,  $\sigma_d(\zeta_d) = [z_{1,x}^2, z_{1,y}^2, z_{1,\varphi}^2, \theta^2, z_{1,y}\theta, z_{1,\varphi}\theta, z_{1,r}\theta]^T$ ,  $\sigma_v(\zeta_v) = [z_1^T z_1, z_1^T z_2, z_2^T z_2]^T$ . The virtual leader is driven to moving along a desired parameterized path  $\eta_r(\theta) = [80 \cos(\theta), -80 \sin(\theta), -\theta]^T$  with  $v_s = 0.015$ . The fault considered herein is settled as follows

$$\begin{cases} \sigma = \text{diag}\{0.19, 0.185, 0.4\}, \bar{\tau} = [1, 1, 0.01]^T, t \in [5, 60] \\ \sigma = \text{diag}\{0.65, 0.72, 0.77\}, \bar{\tau} = [1, 1, 0.01]^T, t \in [180, +\infty) \end{cases}$$

At first, the proposed fault-tolerant control law will be compared with an existing kinetic control law for path maneuvering in Zhang et al. (2021) to show the necessity of the fault-tolerant control mechanism. The compared controller consists of a concurrent learning-based neural predictor (28), (29) and (30), kinematic control law (8), tracking differentiator (9), and the following kinetic control law

$$\tau_a = -K_2 z_2 - \hat{f} + v_a^d$$

where  $K_2 \in \mathbb{R}^{3 \times 3}$  denotes a control gain in the kinetics level. In the simulation, we let  $K_2 = \text{diag}\{5, 5, 5\}$ .

Simulation results are depicted in the following figures. The output trajectory of the ASV is shown in Fig. 4. The path maneuvering error at the kinematic level is shown in Fig. 5. As shown in Figs. 4 and 5, although the ASV is subject to unexpected fault, the geometric objective of path maneuvering can be achieved by using the proposed control method. Fig. 6 depicts the comparisons of output trajectories using the proposed method and the compared kinetic control law in Zhang et al. (2021). Although the compared method in Zhang et al. (2021) can maintain stable control during the fault occurring, the ASV cannot track the desired heading angle. The disordered heading angle is dangerous in practical applications. Fig. 7 depicts the actual control input. The evolution of the path variable is given in Fig. 8, and it is shown that the proposed method can fulfill the dynamic objective of path maneuvering. The learning profile of the neural network using the proposed method is shown in Fig. 9, and the identification of unknown fault coefficients is shown in Fig. 10. It can be observed that the learning profile of the neural network is only slightly affected by the unexpected fault because the proposed method can estimate fault coefficients.

Then, the proposed fault-tolerant control law will be compared with an existing adaptive fault-tolerant kinetic control law for path maneuvering in Lu et al. (2021) to show the efficacy of the proposed method. The compared controller consists of a concurrent learning-based neural predictor (28), (29), and (30), kinematic control law (8), tracking differentiator (9) and the following kinetic control law

$$\begin{cases} \tau_i = -B_i (\hat{\lambda}_i \Psi_i + k_{2,i}) z_{2,i}, i = \bar{u}, \bar{v}, r \\ \dot{\hat{\lambda}}_i = \Gamma_{\hat{\lambda}_i} [\Psi_i z_{2,i}^2 - d_i (\hat{\lambda}_i - \hat{\lambda}_i(0))] \\ \Psi_i = \frac{\|\varphi_i(\zeta_i)\|^2 + 1 + |v_{a,i}|^2}{2b_2} \end{cases}$$

where  $[z_{2,\bar{u}}, z_{2,\bar{v}}, z_{2,r}]^T = z_2$ ,  $[v_{a,\bar{u}}, v_{a,\bar{v}}, v_{a,r}]^T = v_a$ ,  $\text{diag}\{k_{2,\bar{u}}, k_{2,\bar{v}}, k_{2,r}\} \in \mathbb{R}^{3 \times 3}$  denotes a control gain in the kinetics level,  $B_i \in \mathbb{R}^+$  is a parameter

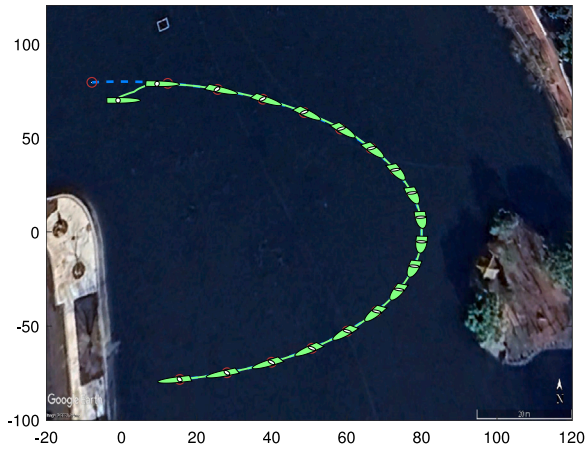


Fig. 4. Output trajectories of the ASV using the proposed method.

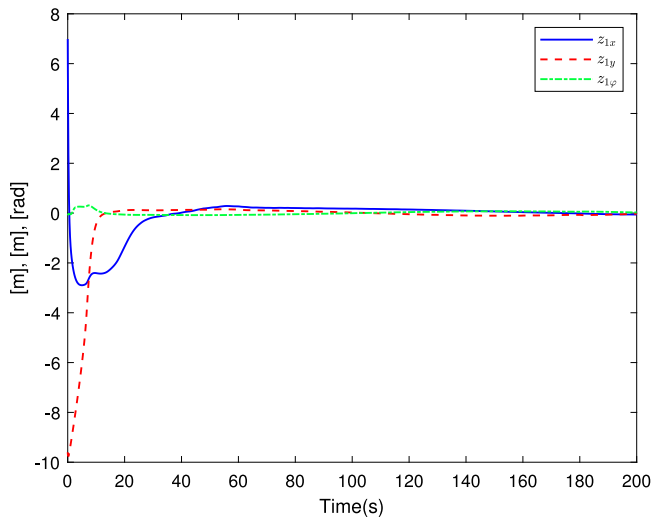


Fig. 5. Kinematic tracking error of the ASV using the proposed method.

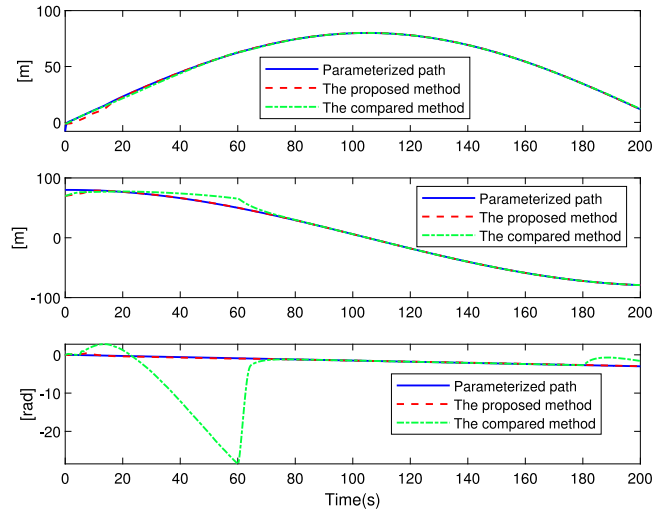


Fig. 6. Comparisons of output trajectories between two methods.

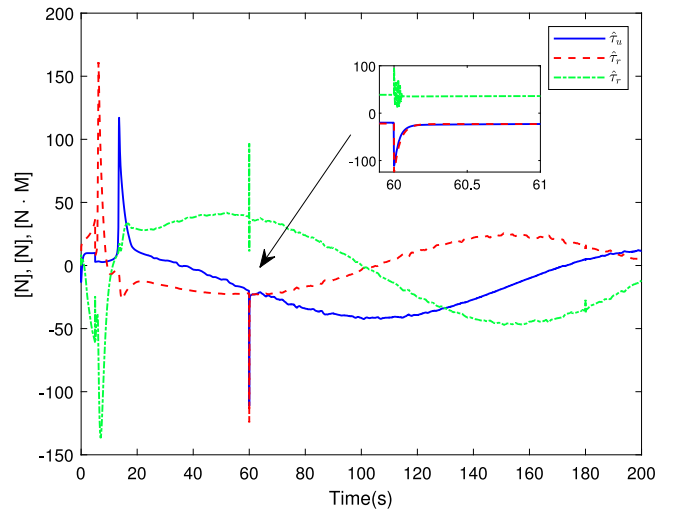


Fig. 7. Actual control input of the ASV using the proposed method.

related to the fault and can be determined by satisfying *Assumption 4* in Lu et al. (2021),  $\Gamma_{\hat{\lambda}_i} \in \mathbb{R}^+$  denotes an adaptation gain for  $\hat{\lambda}_i$ , and  $d_i \in \mathbb{R}^+$  and  $b_2 \in \mathbb{R}^+$  denote tuning parameters. In the simulation, we let  $B_{\bar{u}} = B_{\bar{v}} = 15$ ,  $B_r = 50$ ,  $B_{\bar{u}} = B_{\bar{v}} = 10$ ,  $B_r = 15$ ,  $\Gamma_{\hat{\lambda}_{\bar{u}}} = \Gamma_{\hat{\lambda}_{\bar{v}}} = \Gamma_{\hat{\lambda}_r} = 20$ ,  $d_{\bar{u}} = d_{\bar{v}} = d_r = 0.005$ ,  $b_2 = 0.4$ .

Fig. 11 depicts the comparisons of output trajectories using the proposed method and the compared kinetic control law in Lu et al. (2021). Compared with the control method without fault tolerance in Zhang et al. (2021), it can be observed from Figs. 6 and 11 that the control method in Lu et al. (2021) is able to fault tolerance. However, the performance of the proposed control method is better than the compared method in Lu et al. (2021). Besides, the proposed method does not need *Assumption 4* in Lu et al. (2021).

## 6. Conclusions

A robust adaptive fault-tolerant control method for path maneuvering of the ASV was presented based on a noncooperative game approach in this paper. Two noncooperative game scenarios were considered. The kinematic control and the path update constituted a noncooperative game, and the kinetic control and the unexpected total disturbances also constituted a noncooperative game. The kinematic control law was developed by utilizing an improved dynamic surface control approach. The path update law and the kinetic control law

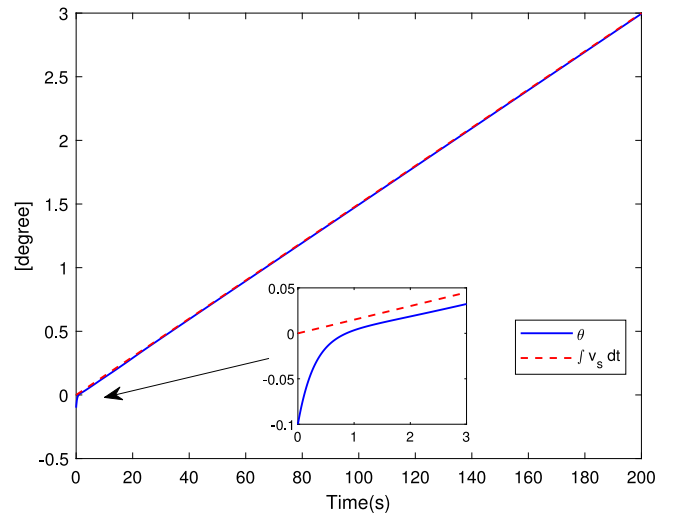


Fig. 8. Evolution of path variable using the proposed method.

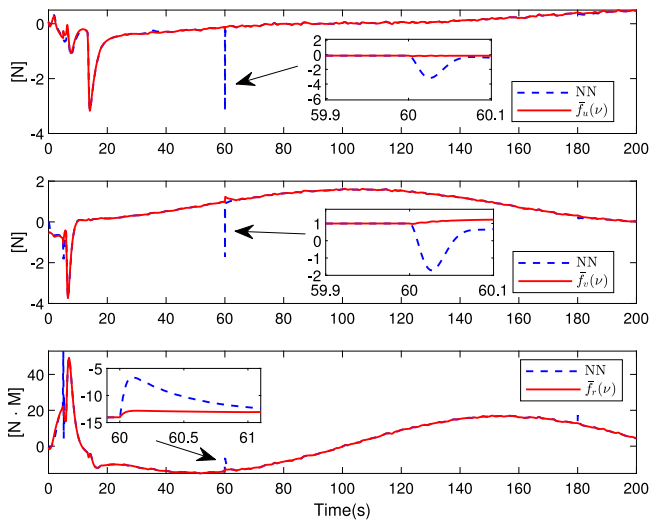


Fig. 9. Learning profile of neural network using the proposed method.

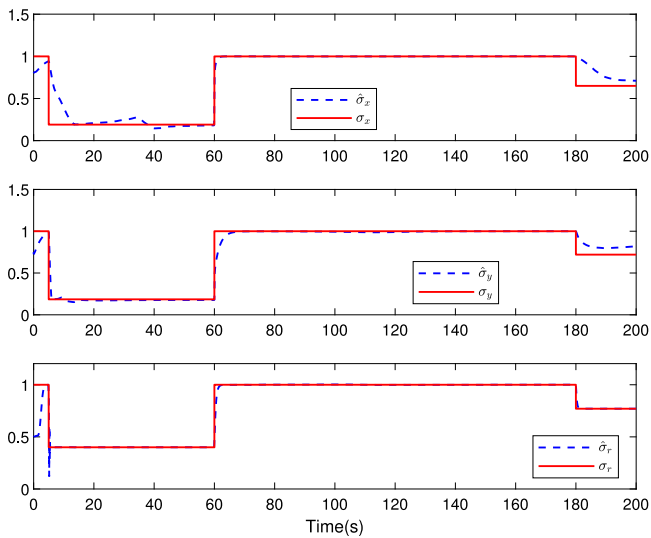


Fig. 10. Identification of unknown fault coefficients using the proposed method.

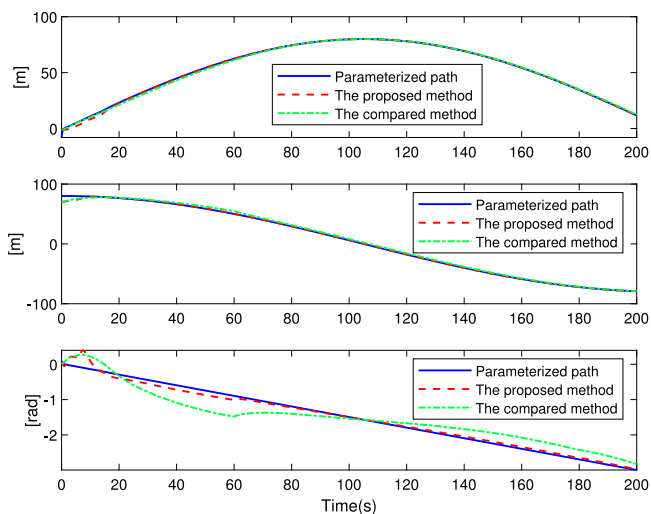


Fig. 11. Comparisons of output trajectories between two methods.

were calculated by using an adaptive dynamic programming approach. Besides, an improved neural predictor was employed as the approximator at the kinetic level. The stability of the closed-loop system was analyzed. The proposed control method was validated on simulation examples. The proposed method could drive the ASV to track the parameterized path regardless of actuator faults, which validated the proposed robust adaptive fault-tolerant path maneuvering controller.

**CRedit authorship contribution statement**

**Yibo Zhang:** Data curation, Funding acquisition, Software, Validation, Visualization, Writing – original draft, Writing – review & editing. **Di Wu:** Investigation, Methodology, Resources, Software. **Peng Cheng:** Investigation, Methodology, Resources, Software. **Wentao Wu:** Investigation, Methodology, Resources, Software. **Weidong Zhang:** Conceptualization, Funding acquisition, Investigation, Methodology, Project administration, Supervision.

**Declaration of competing interest**

The authors declare that they have no known competing financial interests or personal relationships that could have appeared to influence the work reported in this paper.

**Data availability**

No data was used for the research described in the article.

**Acknowledgments**

This work was supported by the National Key R&D Program of China under Grant 2022ZD0119900, the Shanghai Science and Technology Program, China under Grant 22015810300, the Hainan Province Science and Technology Special Fund, China under Grant ZDYF2021GXJS041, the China Post-Doctoral Science Foundation under Grant 2022M722053, the Oceanic Interdisciplinary Program of Shanghai Jiao Tong University, China under Grant SL2022PT112, and the National Natural Science Foundation of China under Grants 52201369 and U2141234.

**References**

Chowdhary, G., Yucelen, T., Mühlegg, E.N., 2013. Concurrent learning adaptive control of linear systems with exponentially convergent bounds. *Internat. J. Adapt. Control Signal Process.* 27, 280–301.

Dacic, D.B., Subbotin, M.V., Kokotovic, P.V., 2006. Control effort reduction in tracking feedback laws. *IEEE Trans. Autom. Control* 51, 1831–1837. <http://dx.doi.org/10.1109/TAC.2006.883064>.

Fossen, T.I., 2011. *Handbook of Marine Craft Hydrodynamics and Motion Control*. John Wiley & Sons.

Gao, S., Peng, Z., Liu, L., Wang, D., Han, Q.L., 2023. Fixed-time resilient edge-triggered estimation and control of surface vehicles for cooperative target tracking under attacks. *IEEE Trans. Intell. Veh.* 8, 547–556. <http://dx.doi.org/10.1109/TIV.2022.3184076>.

Gao, S., Peng, Z., Liu, L., Wang, H., Wang, D., 2021. Coordinated target tracking by multiple unmanned surface vehicles with communication delays based on a distributed event-triggered extended state observer. *Ocean Eng.* 227, 108283. <http://dx.doi.org/10.1016/j.oceaneng.2020.108283>.

Gu, N., Wang, D., Peng, Z., Wang, J., 2021. Safety-critical containment maneuvering of underactuated autonomous surface vehicles based on neurodynamic optimization with control barrier functions. *IEEE Trans. Neural Netw. Learn. Syst.* 1–14. <http://dx.doi.org/10.1109/TNNLS.2021.3110014>.

Gu, N., Wang, D., Peng, Z., Wang, J., Han, Q.L., 2022a. Advances in line-of-sight guidance for path following of autonomous marine vehicles: An overview. *IEEE Trans. Syst. Man Cybern.: Syst.* <http://dx.doi.org/10.1109/TSMC.2022.3162862>.

Gu, N., Wang, D., Peng, Z., Wang, J., Han, Q.L., 2022b. Disturbance observers and extended state observers for marine vehicles: A survey. *Control Eng. Pract.* 123, 105158. <http://dx.doi.org/10.1016/j.conengprac.2022.105158>, URL <https://www.sciencedirect.com/science/article/pii/S0967066122000624>.

Guo, B.Z., Zhao, Z.L., 2011. On convergence of tracking differentiator. *Internat. J. Control* 84, 693–701. <http://dx.doi.org/10.1080/00207179.2011.569954>.

- Hao, L.Y., Zhang, H., Li, H., Li, T.S., 2020. Sliding mode fault-tolerant control for unmanned marine vehicles with signal quantization and time-delay. *Ocean Eng.* 215, 107882. <http://dx.doi.org/10.1016/j.oceaneng.2020.107882>.
- He, S., Dai, S.L., Zhao, Z., Zou, T., Ma, Y., 2023. UDE-based distributed formation control for MSVs with collision avoidance and connectivity preservation. *IEEE Trans. Ind. Inform.* 1–12. <http://dx.doi.org/10.1109/TII.2023.3274234>.
- Hu, B.B., Zhang, H.T., 2022. Bearing-only motional target-surrounding control for multiple unmanned surface vessels. *IEEE Trans. Ind. Electron.* 69, 3988–3997. <http://dx.doi.org/10.1109/TIE.2021.3076719>.
- Jiang, Y., Peng, Z., Liu, L., Wang, D., Zhang, F., 2023. Safety-critical cooperative target enclosing control of autonomous surface vehicles based on finite-time fuzzy predictors and input-to-state safe high order control barrier functions. *IEEE Trans. Fuzzy Syst.* <http://dx.doi.org/10.1109/TFUZZ.2023.3309706>.
- Jin, X., 2016. Fault tolerant finite-time leader–follower formation control for autonomous surface vessels with los range and angle constraints. *Automatica* 68, 228–236. <http://dx.doi.org/10.1016/j.automatica.2016.01.064>.
- Khalil, H.K., 2015. *Nonlinear Control*. Pearson Education.
- Krstic, M., Kanellakopoulos, I., Kokotovic, P.V., 1995. *Nonlinear and Adaptive Control Design*. John Wiley & Sons.
- Liu, L., Wang, D., Peng, Z., Han, Q.L., 2021. Distributed path following of multiple under-actuated autonomous surface vehicles based on data-driven neural predictors via integral concurrent learning. *IEEE Trans. Neural Netw. Learn. Syst.* 32, 5334–5344. <http://dx.doi.org/10.1109/TNNLS.2021.3100147>.
- Liu, L., Wang, D., Peng, Z., Li, T., Chen, C.L.P., 2020. Cooperative path following ring-networked under-actuated autonomous surface vehicles: Algorithms and experimental results. *IEEE Trans. Cybern.* 50, 1519–1529.
- Lu, Y., Xu, X., Qiao, L., Zhang, W., 2021. Robust adaptive formation tracking of autonomous surface vehicles with guaranteed performance and actuator faults. *Ocean Eng.* 237, 109592. <http://dx.doi.org/10.1016/j.oceaneng.2021.109592>.
- Lv, G., Peng, Z., Li, Y., Liu, L., Wang, D., 2023. Barrier-certified model predictive cooperative path following control of connected autonomous surface vehicles. *IEEE Trans. Netw. Sci. Eng.* 1–13. <http://dx.doi.org/10.1109/TNSE.2023.3260259>.
- Lv, M., Peng, Z., Wang, D., Han, Q.L., 2022. Event-triggered cooperative path following of autonomous surface vehicles over wireless network with experiment results. *IEEE Trans. Ind. Electron.* 69, 11479–11489. <http://dx.doi.org/10.1109/TIE.2021.3120442>.
- Ma, Y., Meng, Q., Jiang, B., Ren, H., 2023. Fault-tolerant control for second-order nonlinear systems with actuator faults via zero-sum differential game. *Eng. Appl. Artif. Intell.* 123, 106342. <http://dx.doi.org/10.1016/j.engappai.2023.106342>.
- Ma, L., Wang, Y.L., Han, Q.L., 2022. Cooperative target tracking of multiple autonomous surface vehicles under switching interaction topologies. *IEEE/CAA J. Autom. Sin.* <http://dx.doi.org/10.1109/JAS.2022.105509>.
- Ma, Y., Zhu, G., Li, Z., 2019. Error-driven-based nonlinear feedback recursive design for adaptive trajectory tracking control of surface ships with input saturation. *IEEE Intell. Transp. Syst. Mag.* 11, 17–28. <http://dx.doi.org/10.1109/MITS.2019.2903517>.
- Peng, Z., Wang, D., Li, T., Han, M., 2020. Output-feedback cooperative formation maneuvering of autonomous surface vehicles with connectivity preservation and collision avoidance. *IEEE Trans. Cybern.* 50, 2527–2535.
- Peng, Z., Wang, J., Wang, D., 2018. Distributed maneuvering of autonomous surface vehicles based on neurodynamic optimization and fuzzy approximation. *IEEE Trans. Control Syst. Technol.* 26, 1083–1090.
- Ren, H., Jiang, B., Ma, Y., 2022. Zero-sum differential game-based fault-tolerant control for a class of affine nonlinear systems. *IEEE Trans. Cybern.* 1–11. <http://dx.doi.org/10.1109/TCYB.2022.3215716>.
- Skjetne, R., Fossen, T.I., Kokotović, P.V., 2004. Robust output maneuvering for a class of nonlinear systems. *Automatica* 40, 373–383. <http://dx.doi.org/10.1016/j.automatica.2003.10.010>.
- Skjetne, R., Fossen, T.I., Kokotović, P.V., 2005. Adaptive maneuvering, with experiments, for a model ship in a marine control laboratory. *Automatica* 41, 289–298.
- Wang, H., Tan, H., Peng, Z., 2024. Quantized communications in containment maneuvering for output constrained marine surface vehicles: Theory and experiment. *IEEE Trans. Ind. Electron.* 71, 880–889. <http://dx.doi.org/10.1109/TIE.2023.3241256>.
- Wu, W., Peng, Z., Liu, L., Wang, D., 2022a. A general safety-certified cooperative control architecture for interconnected intelligent surface vehicles with applications to vessel train. *IEEE Trans. Intell. Veh.* 7, 627–637. <http://dx.doi.org/10.1109/IV.2022.3168974>.
- Wu, W., Tong, S., 2023. Fixed-time formation fault tolerant control for unmanned surface vehicle systems with intermittent actuator faults. *Ocean Eng.* 281, 114813. <http://dx.doi.org/10.1016/j.oceaneng.2023.114813>.
- Wu, W., Zhang, Y., Zhang, W., Xie, W., 2022b. Distributed finite-time performance-prescribed time-varying formation control of autonomous surface vehicles with saturated inputs. *Ocean Eng.* 266, 112866. <http://dx.doi.org/10.1016/j.oceaneng.2022.112866>.
- Zhang, G., Deng, Y., Zhang, W., 2017. Robust neural path-following control for underactuated ships with the DVS obstacles avoidance guidance. *Ocean Eng.* 143, 198–208.
- Zhang, G., Liu, S., Huang, J., Zhang, W., 2022. Dynamic event-triggered path-following control of underactuated surface vehicle with the experiment verification. *IEEE Trans. Veh. Technol.* 71, 10415–10425. <http://dx.doi.org/10.1109/TVT.2022.3184305>.
- Zhang, Y., Wang, D., Yin, Y., Peng, Z., 2021. Event-triggered distributed coordinated control of networked autonomous surface vehicles subject to fully unknown kinetics via concurrent-learning-based neural predictor. *Ocean Eng.* 234, 108966. <http://dx.doi.org/10.1016/j.oceaneng.2021.108966>.
- Zhang, Y., Wu, W., Zhang, W., 2023. Noncooperative game-based cooperative maneuvering of intelligent surface vehicles via accelerated learning-based neural predictors. *IEEE Trans. Intell. Veh.* 8, 2212–2221. <http://dx.doi.org/10.1109/IV.2022.3222009>.
- Zhu, G., Ma, Y., Hu, S., 2023. Event-triggered adaptive PID fault-tolerant control of underactuated asvs under saturation constraint. *IEEE Trans. Syst. Man Cybern.: Syst.* 53, 4922–4933. <http://dx.doi.org/10.1109/TSMC.2023.3256538>.